Efficient Photo-Hole Injection from Adsorbed Cyanine Dyes into Electrodeposited Copper(I) Thiocyanate Thin Films

Brian O'Regan*,† and Daniel T. Schwartz*,‡

Department of Chemistry and Department of Chemical Engineering, University of Washington, Seattle, Washington 98195

Received January 31, 1995. Revised Manuscript Received April 21, 1995®

Photocurrent action spectra and current/voltage characteristics are presented for transparent thin films of p-type CuSCN immersed in ethanol electrolytes containing cyanine dyes. The action spectra show that the photocurrent is caused by hole injection from adsorbed dyes. Of the dyes tested, those with oxidation potentials ≥0.7 V vs SCE photoinject holes into CuSCN with quantum efficiencies greater than 50%. The highest quantum efficiency measured was ≥80%. From the threshold oxidation potential for injection and the photocurrent onset potential, the valence band edge of CuSCN in ethanol/TBABF$_4$ is estimated to lie between 0.55 and 0.75 V vs SCE. The results suggest that CuSCN is a promising candidate material for the hole-conducting portion of dye sensitized heterojunctions for solar photovoltaic applications.

Introduction

Recent studies of dye-sensitized photoelectrochemical (DSPEC) solar cells report energy efficiencies as high as 10%.[1,2] These new DSPEC cells are based on porous high-surface-area TiO$_2$ electrodes in contact with redox couples in low-vapor-pressure organic solvents. The TiO$_2$ is sensitized to visible radiation with a monolayer of adsorbed dye that is present on all of the internal surface area; thus many monolayers of dye intercept the incident light, allowing for complete absorption and utilization. When photoexcited, the dye transfers an electron to the TiO$_2$ and a positive charge to the redox couple. Because light is absorbed only in the dye layer, there are no photogenerated electrons and holes in the same material, thus bulk electron–hole recombination cannot occur. The absence of bulk recombination relaxes the materials purity requirements for DSPEC cells, relative to other solar cells, leading to a low cost of fabrication.

However, there are a number of scientific and technological hurdles that must be overcome to make current DSPEC solar cell designs commercially viable. One of the problem areas is the containment and longevity of the liquid-phase electrolyte.[3] Replacing the electrolyte with a solid material with appropriate charge-transport characteristics will circumvent the problems associated with liquids. Ideally, an all-solid-state DSPEC cell consists of a transparent high-surface-area electron-conducting material such as TiO$_2$, whose pore structure is filled with a transparent hole conductor. A layer of visible-light-absorbing dye, inside the pores, at the interface between the electron and hole conductors, photoinjects electrons into the electron conductor and is regenerated by injecting holes into the hole conductor. This structure is, in effect, no longer electrochemical and may be more properly called a dye-sensitized heterojunction (DSH). Figure 1 illustrates the energetics of a DSH utilizing TiO$_2$ and a p-type semiconductor as the hole-transport layer.

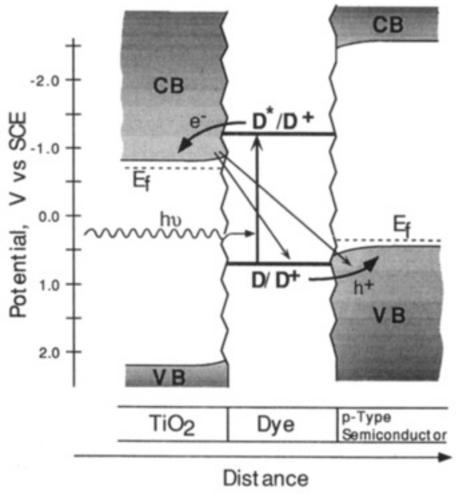

Figure 1. Energy/position schematic for a planar dye-sensitized heterojunction (DSH) formed from TiO$_2$ and a p-type semiconductor. The dye is drawn with a transition energy of 1.9 eV, corresponding to an absorption edge of 650 nm. D/D$^+$ indicates the dye oxidation potential and D*/D$^+$ the "reducing potential"[30] of the excited dye. It is assumed here that electron injection precedes hole injection. Desired electron and hole flow are shown as thick arrows; recombination of the electron in TiO$_2$ with the dye cation or with the hole are shown as thin arrows. In a high-surface-area DSH, the TiO$_2$ would be porous, the dye would coat the inside of the pores, and the p-type semiconductor would fill the pores.

To be a viable candidate for a DSH cell, a prospective hole conductor must have low optical absorption in the visible portion of the spectrum (≤0.05 absorbance units for a 10 μm film), reasonable hole conductivity (≥5 × 10^{-4} S cm^{-1}), and a very low rate of photodegradation. In addition it must be energetically and kinetically feasible for dyes to efficiently inject charge carriers into the hole conductor and the electron conductor used. This condition places restrictions on the oxidation potential

---

[†] Department of Chemistry.

[‡] Department of Chemical Engineering.

® Abstract published in *Advance ACS Abstracts,* June 1, 1995.

(1) Nazeeruddin, M. K.; Kay, A.; Rodicio, I.; Humphry-Baker, R.; Muller, E.; Liska, P.; Vlachopoulos, N.; Gratzel, M. *J. Am. Chem. Soc.* **1993**, *115*, 6382.

(2) O'Regan, B.; Gratzel, M. *Nature* **1991**, *353*, 737.

(3) Gratzel, M.; Kay, A.; Liska, P., personal communication.

0897-4756/95/2807-1349$09.00/0

of the hole-transport layer (e.g., the valence band edge of a p-type semiconductor). For example, to be compatible with the band edge potential of TiO_2, and dyes which are known to sensitize TiO_2, the valence band edge potential of the hole conductor must be less than 800 mV vs SCE. Once a hole conductor with the above properties is identified, a deposition strategy is needed to fill the nanoporous TiO_2 electrodes with the selected material while maintaining the integrity of the dye monolayer present on the TiO_2 surface.

We have selected the Cu(I) pseudo-halide CuSCN, a wide-bandgap p-type semiconductor, as a promising hole-conducting material.[4,5] Hole injection from excited rhodamine B and methyl violet into CuSCN is known to occur for films grown anodically on copper sheet, however, these experiments have yielded quantum efficiencies less than 50%.[6-8] To be able to deposit CuSCN into the pores of TiO_2, we have developed methods for electrodepositing CuSCN onto metal and conductive oxide (SnO_2) surfaces.[9] We report below on experiments designed to characterize these electrodeposited films with respect to hole injection and valence band-edge potential.

For these experiments we have used a series of cyanine dyes with oxidation potentials ranging from 400 mV to 1.1 V vs SCE. Although cyanine dyes are almost certainly too unstable to use in an eventual solar application, a large amount is known about their behavior on the surface of silver halides (AgX), due to their extensive application in photography.[10,11] All the dyes in this study are known to sensitize the formation of latent image in AgX.[12] The sensitization of latent image formation is thought to begin with electron injection from the dye into the AgX conduction band or perhaps subconduction band states.[13] Several of the dyes are known to sensitize latent image formation with an absorbed photon quantum efficiency approaching 1.[14] Moreover, some of the dyes are also known to inject holes into AgX as evidenced by their ability to sensitize direct positive formation in internally fogged AgX emulsions.[15]

Sensitized hole injection has been studied on substrates of AgX, molecular crystals, and hole conductors used in xerography.[15-19] Only a few studies have been done on dye-sensitized hole injection into inorganic semiconductors other than AgX; for example, GaP,[20] SiC,[21] PbI_2,[22] CuI,[23] CuSCN,[6-8] BiOCl,[24] and Si.[25] In all cases the solvent has been water (or undried air in the case of photopotential or photographic studies). The maximum reported hole injection efficiency that we are aware of is approximately 30%. This paper reports the first measurements of very high quantum efficiency dye-sensitized hole injection into a semiconductor.

Experimental Section

Cyanine dyes 1,1′-diethyl-2,2′-cyanine iodide (DCI) and 3,3′-diethyloxacarbocyanine iodide (DOCCI) were purchased from Aldrich. Cyanine dyes 3,3′-diethyloxadicarbocyanine iodide (DODCI), 1,1′-diethyl-2,2′-carbocyanine chloride (PCCl, also known as pinacyanol), 1,1′-diethyl-4,4′-carbocyanine iodide (CCI, also known as cryptocyanine), neocyanine iodide (NCI), and 3,3′-diethyl-4,5,4′,5′-dibenzothiacarbocyanine bromide (ES-ABr also known as Ethyl-Stains-All) were purchased from Kodak. Salts and solvents were ordered from various sources. Salts were used as delivered. Solvents were dried over Fluka molecular sieve. For electrochemical studies, neocyanine iodide was changed to the hexafluorophosphate salt by precipitation from water with ammonium hexafluorophosphate.

Electrodeposition of CuSCN was carried out with a Cypress Systems Omni 90 potentiostat connected to a three-electrode electrochemical cell containing 6 mL of the electrodeposition solution (described below). CuSCN was deposited on the lower 1 cm of 1 × 3 cm transparent conductive SnO_2–glass electrodes (Asahi TCO–glass, conductive layer: 0.5 μm fluorine doped SnO_2). The counter electrode was a 1.5 × 1.5 cm platinum sheet positioned parallel to the working electrode at a distance of 1 cm. A platinum wire pseudo reference electrode was used. Just prior to electrodeposition, the SnO_2–glass electrodes were heated in air for 15 min at 400 °C in order to remove adsorbed organic material and water.

Transparent CuSCN thin films for photoelectrochemical measurements were electrodeposited onto SnO_2 from 0.1 M $Cu(BF_4)_2$, 0.025 M KSCN in ethanol. Deposition was carried out potentiostatically, normally at a voltage of −700 mV vs the platinum pseudoreference. (In this solution the platinum pseudoreference gives a stable potential of 660 ± 20 mV vs SCE.) For the purposes of this study, where we quantify the amount of dye present by transmission spectroscopy, it is necessary that the CuSCN films be optically smooth. CuSCN films deposited from freshly mixed $Cu(BF_4)_2$/KSCN solutions are very rough on a 1 μm scale and are sufficiently scattering that they are opaque. We have found that storing (aging) the electrodeposition solution 4–6 days results in films which are much smoother. For film thicknesses up to 1 μm, CuSCN films deposited from this aged solution are transparent. Further study of this effect is underway and will be published in a subsequent paper.[9] After removal from the deposition solution, the electrodes were rinsed in ethanol, blown dry under a stream of air, and stored in air under normal interior light levels.

Photoelectrochemical measurements were made in a flat-sided three-electrode cell containing 5 mL of 0.05 M tetrabutylammonium tetrafluoroborate in ethanol. Dye and LiI were added to the solution as noted below. The counter electrode was a platinum sheet and the reference electrode was a platinum wire. All potentials reported below are in volts vs SCE. The cell was isolated from the atmosphere to prevent water contamination. No attempt was made to remove oxygen as it acts as the electron acceptor regenerating the photoreduced dye (see discussion). The transparent CuSCN working

---

(4) Melendres, C. A.; O'Leary, T. J.; Solis, J. *Electrochim. Acta* **1991**, *36*, 505.

(5) Son, Y.; de Taconi, N. R.; Rajeshwar, K. *J. Electroanal. Chem.* **1993**, *345*, 135.

(6) Tennakone, K.; Kahanda, M.; Kasige, C.; Abeysooriya, P.; Wijayanayaka, R. H.; Kaviratna, P. *J. Electrochem. Soc.* **1984**, *131*, 1574.

(7) Tennakone, K.; Fernando, C. A. N.; Dewasurendra, M. *J. Photochem.* **1987**, *38*, 75.

(8) Fernando, C. A. N.; Kitagawa, A.; Suzuki, M.; Takahashi, K.; Komura, T. *Sol. Energy Mater. Sol. Cells* **1994**, *33*, 301.

(9) O'Regan, B.; Schwartz, D. T. In *Symposium on Nanostructured Materials in Electrochemistry*; Meyes, G. J., Searson, P. C., Eds.; Electrochemical Society: Pennington, NJ, 1995.

(10) West, W.; Carroll, B. H. *J. Chem. Phys.* **1947**, *15*, 529.

(11) Spitler, M. T. *J. Imag. Sci.* **1991**, *35*, 351.

(12) Brooker, L. G. S. In *The Theory of the Photographic Process*; James, T. H., Ed.; Macmillan: New York, 1966; p 198.

(13) Gilman, P. B.; Evans, F. J.; Koszelak, T. D. *Photogr. Sci. Eng.* **1977**, *21*, 296.

(14) Carroll, B. H. *Introduction to Photographic Theory*; John Wiley: New York, 1980.

(15) Berriman, R. W.; Gilman, P. B. *Photogr. Sci. Eng.* **1973**, *17*, 235.

(16) Auweraer, V. d.; M., B. V.; Biesmans, G.; Schryver, F. C. D.; Willig, F. *Langmuir* **1987**, *3*, 992.

(17) Gerischer, H.; Selzle, H. *Electrochim. Acta* **1973**, *18*, 799.

(18) Sandifer, J. R. *J. Imag. Sci.* **1985**, *29*, 27.

(19) Umeda, M.; Hashimoto, M. *J. Appl. Phys.* **1992**, *72*, 117.

(20) Memming, R.; Tributsch, H. *J. Phys. Chem.* **1971**, *75*, 562.

(21) Memming, R. *Photochem. Photobiol.* **1972**, *16*, 325.

(22) Levy, B.; Dickson, C. R. *Photog. Sci. Eng.* **1975**, *19*, 79.

(23) Tennakone, K.; Fernando, C. A. N.; Dewasurendra, M.; Kariappert, M. S. *Jpn. J. Appl. Phys.* **1987**, *26*, 561.

(24) Poznyak, S. K.; Kulak, A. I. *Electrochim. Acta* **1990**, *35*, 1941.

(25) Gratzel, M.; Frei, H. *J. Phys. Chem.* **1989**, *93*, 7037.

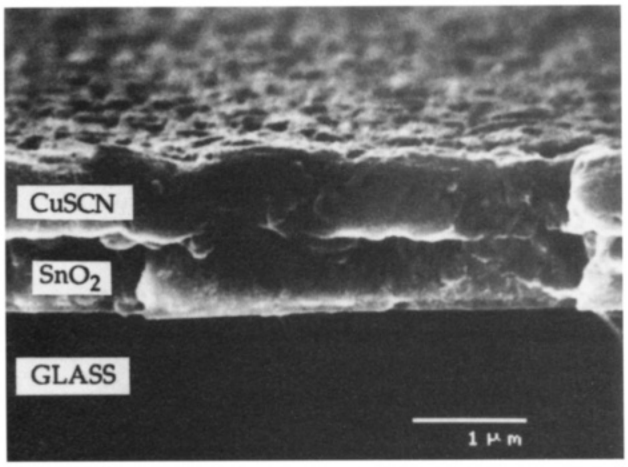

Figure 2. Scanning electron micrograph showing the cross section and surface of an electrodeposited transparent CuSCN film on SnO_2-coated glass.

electrode was positioned with its back against the illuminated side of the cell, "rear illumination", so that light reaching the CuSCN layer did not pass through the solution.

Illumination was provided with a 150 W xenon lamp (Oriel) focused through a 10 cm water filter and a Jobin Yvon H-20 0.2 m monochromator. A 550 nm cutoff filter was used when illuminating with wavelengths longer than 700 nm. When working above 800 nm the monochromator was illuminated with a 500 W tungsten halogen source to avoid the 824 peak in the xenon lamp output. Light intensity was measured with a Tektronix J1812 irradiance head. For efficiency measurements, the center of the 1 cm^2 electrode was illuminated with a 3 mm diameter collimated beam from the monochromator. Typical monochromatic photon flux was 100−200 $\mu W/cm^2$, equivalent to 4−8 μA of photons incident on the illuminated spot. The photocurrent was measured as the difference between the dark and illuminated current about 1 s after the onset of illumination. Photocurrents were measured with the electrodes biased approximately 50 mV positive of the open-circuit potential in the dark, resulting in a few tens of nanoamperes of anodic dark current. At this potential any CuSCN bulk photoconductivity will result in an increase in the anodic current, whereas the dye-sensitized photocurrent is cathodic. Thus any measured cathodic current resulting from illumination does not stem from increased conductivity of the CuSCN. Typical photocurrents were between 0.1 and 1 μA.

Absorption spectra were taken using an HP 8452A spectrometer with the beam masked to 3 mm diameter and with the electrode positioned so that the absorption spectra corresponded to the same spot that was illuminated during the photoelectrochemistry. Spectra of the dye adsorbed to the transparent CuSCN electrodes were taken by removing the electrode from the dye solution and quickly patting dry with clean adsorbent paper. This was done to remove the dye-containing ethanol before it could evaporate and thereby deposit more dye onto the electrode. Preliminary tests showed that this method resulted in less than a 5% increase in the amount of adsorbed dye relative to the amount which was adsorbed in solution. The amount of dye adsorbed was measured by subtracting the absorption spectra of the nondyed electrode from that of the electrode with dye. Typical electrodes absorbed between 3 and 12% of the incident photon flux. Small changes in the position of the electrodes resulted in interference fringes in the subtracted spectra. When necessary these fringes were subtracted from the absorption spectra. The fringes limited the accuracy of the dye measurement to approximately ±7%. Micrographs were acquired with a JEOL 5200 SEM.

Results and Discussion

Figure 2 shows the typical morphology of a 1 μm CuSCN film deposited from an aged solution. The surface roughness is on the order of 300 nm and is too low to strongly scatter visible light. To the eye, these films are completely transparent and colorless. Figure 3A, spectrum "a", is the absorbance measured in the spectrometer for a 1 μm film on SnO_2. The apparent absorbance above 400 nm is almost entirely due to residual scattering and can be avoided by using thinner films. However, in thinner, more transparent, films, the strong interference fringes that appear make the calculation of the dye spectrum by subtraction more difficult (Figure 3A). By X-ray diffraction the films were found to be composed of the β-crystal form of CuSCN.[26] By comparing the thickness of the films, their weight, and the density of β-CuSCN, we have determined that the films are within 80% of the theoretical density. No porosity was evident at the resolution of the SEM used (see Figure 2). Although this does not preclude porosity at a smaller scale, we believe at this time that the CuSCN films are dense and that the photoelectrochemistry discussed below is occurring on the outer surface.

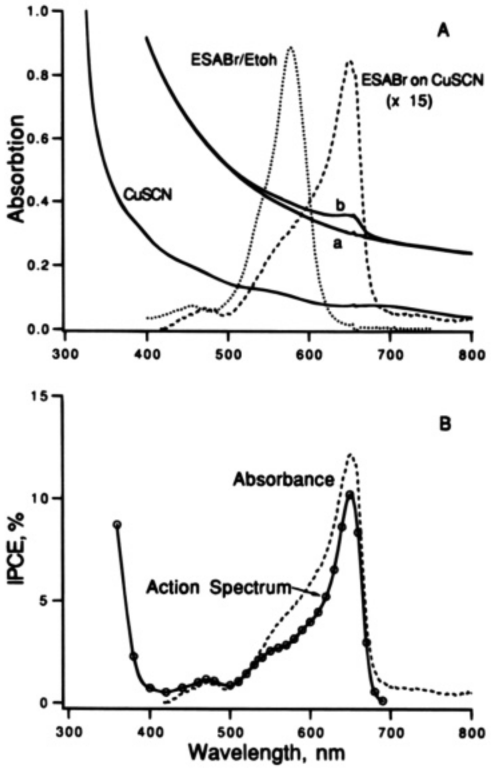

Figure 3. Spectral and photoelectrochemical response of ESABr dye on a CuSCN film deposited on conducting glass. (A) Dashed line: absorption spectrum (×15) of ESABr adsorbed on a 1 μm CuSCN film, as calculated by subtraction of spectrum (a) from (b). Spectrum (a) is that of the bare CuSCN film; (b) is that of the same film with dye. Dotted line: ESABr spectrum in ethanol, arbitrary units. Solid line labeled CuSCN: Absorbance of a CuSCN film calculated by subtraction of the spectrum of bare SnO_2. Undulations result from interference. (B) Points and solid spline: action spectrum plotted as incident photon to current efficiency (IPCE); in ethanol, 6 mM LiI, 10^{-4} M ESABr. Dashed line: absorbance of the dye on the same electrode plotted as percent of light absorbed.

Electrodes were dyed by immersion in 10^{-4} M dye solution. Dye adsorption was essentially complete in less than 1 h; however in the case of aggregated states of the dye, growth, and changes in size of the aggregates continued over longer times. Figure 3A is an example

---

(26) Smith, D. L.; Saunders, V. I. *Acta Crystallogr.* **1981**, *B37*, 1807.

Table 1. Results of Dye Sensitization of CuSCN Films with Cyanine Dyes

dye	$E°_{oxa}$,[a] V vs SSCE	$E°_{red}$,[a] V vs SSCE	λ_{max} in EtOH, nm	λ_{max} I_{phot},[b] nm	hole injection efficiency[c]
DCI	1.11	−1.13	524	540	0.7
DOCCI	1.07	−1.3	485	502	0.6
ESABr	0.77	−1.07	578	(580)[d]	<0.7[d]
ESABr J-agg				641	0.88
PCCl	0.76	−1.04	606	637	0.62
DODCI	0.7	−1.04	560	594	0.65
CCI	0.55	−0.86	708	737	0.2
NCI	0.4		776		<0.05

[a] Oxidation and reduction potentials in acetonitrile from ref 31 except for NCI measured as 1 mM neocyanine hexafluorophosphate in acetonitrile with 0.1 M tetrabutylammonium tetrafluoroborate. [b] Wavelength of maximum quantum efficiency of hole injection. [c] Hole injection efficiency as absorbed photon to current efficiency (APCE, see text). We believe the accuracy of the these numbers to be ±0.1 based on the listed accuracy of the Tektronics irradiance head (±5%), the wander in the lamp intensity (±2%), and our estimate of the inaccuracy of the subtraction used to measure the adsorbed dye (up to ±7%). Because the incident flux used to calculate the APCEs has not been corrected for losses in the SnO_2 or CuSCN, the listed APCEs are all biased low to the same degree (see text). [d] The peak of the monomer action spectra is not know (see Figure 3). The monomer injection efficiency is an upper limit, due to an unknown amount of J-aggregate absorption at 580 nm.

of the CuSCN absorption spectra and the subtraction resulting in the adsorbed dye spectra. Cyanine dyes adsorb only weakly to the surface of CuSCN from ethanol. Addition of millimolar concentrations of I^- or SCN^- to the dye solution increases the amount of dye adsorbed and, in the case of ESABr, favors the formation of the aggregates. Concentrations of halide ion greater than 5 mM often cause detachment of the CuSCN from the SnO_2. Dyed electrodes immersed in dye-free ethanol/$TBABF_4$ solutions lose most of their adsorbed dye and photoelectrochemical response, in less than 10 min; thus we performed the photoelectrochemical experiments in solutions containing 10^{-5} or 10^{-4} M dye. Dye in the solution does not contribute to the photocurrent (see below), and because of the rear illumination dye in the solution does not affect the light intensity at the electrode surface.

Of seven cyanine dyes tested, six sensitized measurable cathodic photocurrents under monochromatic illumination. Table 1 summarizes the results. Figures 3 and 4 show the absorption and photocurrent action spectra for five of the dyes. The photocurrent action spectra show peaks whose characteristics are nearly identical to the absorption spectra of the adsorbed dyes. Both the adsorbed dye spectra and the action spectra are similar to the spectra of the dye in solution, red shifted to some degree. The increase in photocurrent toward 400 nm is due to the intrinsic response of CuSCN and was present when blanks of CuSCN were run without dye. Blanks of bare SnO_2 were run in all dye solutions and showed dye-sensitized photocurrents at least 2 orders of magnitude lower than CuSCN. The bare SnO_2 electrodes also showed ~6 times more cathodic dark current, at −200 mV, than the CuSCN-covered SnO_2. The CuSCN is thus blocking to cathodic current as expected for a p-type semiconductor biased negative of its flat band potential. For a p-type semiconductor, the dye-sensitized photocurrent stems from hole injection by the excited dye into the valence band of the CuSCN, followed by collection of the injected hole at the SnO_2 back contact. The dye is then regenerated by transferring an electron to some electron acceptor in solution. As we have not added an electron acceptor, oxygen is acting as the electron acceptor in these experiments. This is confirmed by the decline in photocurrent when oxygen is removed by nitrogen bubbling and the restoration of the photocurrent by air bubbling.

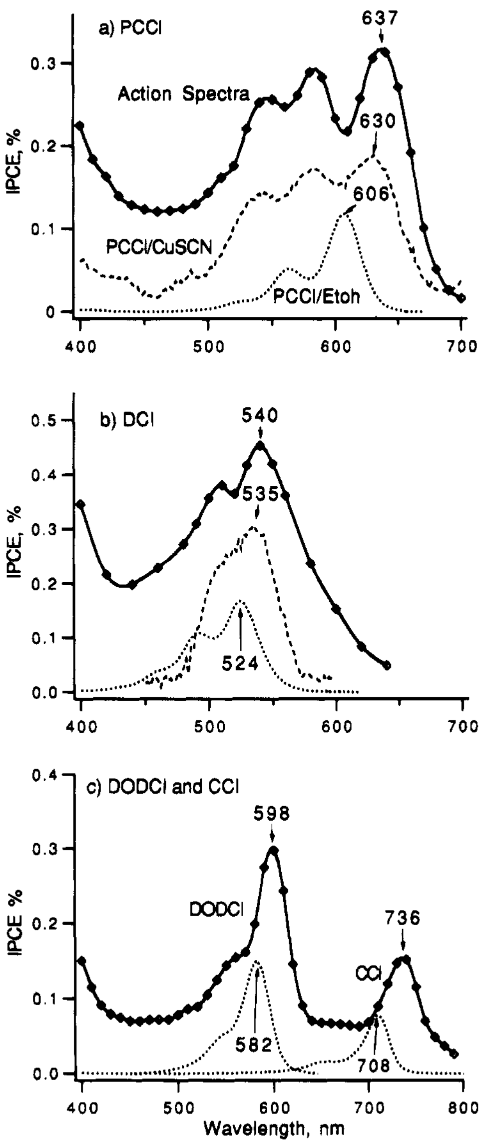

Figure 4. Photoelectrochemical response of cyanine dyes on CuSCN. Points and solid splines: action spectra as IPCE. Dashed lines: absorption spectra of the dye adsorbed to the electrode. Taken dry. Dotted lines: absorption spectra of the dye in ethanol. The absorption spectra are in arbitrary units, scaled for clarity of display. Dyes adsorbed from 10^{-4} M solution. Photoelectrochemical solutions: (a, b) ethanol, 0.05 M $TBABF_4$, no added dye; (c) ethanol, 0.05 M $TBABF_4$, approximately 10^{-5} M in both dyes. The higher relative efficiency of CCI to DODCI here, compared to Table 1, is due to the stronger adsorption of CCI (see text).

In general, cyanine dyes appear to be quite efficient sensitizers for CuSCN. The action spectra in Figures 3 and 4 are plotted as incident photon to current efficiency (IPCE) which is simply the photocurrent divided by the incident photon flux (in microamperes). The efficiencies listed in Table 1 are the absorbed photon to current efficiency (APCE), which is the IPCE divided by the fraction of incident photons absorbed by the dye. The values listed were measured at the peak of the action spectra. The highest APCE we have measured, 88%, is shown by the ESABr aggregate. The APCE can also be expressed as

$$\mathrm{APCE} = \phi_{\mathrm{inj}}\phi_{\mathrm{esc}} = \text{photocurrent } (\mu\mathrm{A}) / (\text{photon flux } (\mu\mathrm{A}) \times \text{absorbance})$$

where ϕ_{inj} is the hole injection efficiency, and ϕ_{esc} is the efficiency with which hole escape to the bulk of the CuSCN competes with recombination across the interface.

For the values in Table 1, the incident flux was corrected for losses in the cell windows but not for reflection or adsorption in either the SnO_2 or CuSCN layers. The SnO_2/glass interface has an antireflective coating of unknown efficacy, and the rough SnO_2/CuSCN interface will reflect and scatter in a manner difficult to model. Taking into account that the escape efficiency, ϕ_{esc}, cannot be larger than 1, and the incident light correction just mentioned, the hole injection efficiency for an excited ESABr aggregate on our electrodes, in ethanol, is certainly greater than 80% and most likely greater than 90%. Because ESABr is not soluble in water, CuSCN electrodes dyed with ESABr from ethanol can be tested in water without added dye. The APCE for ESABr in water is about 20%.

The APCE calculation also assumes that the dye in the solution does not contribute significantly to the photocurrent. This assumption is justified by two observations. First, the photocurrent action spectra for the dyes in Figures 3 and 4 more closely resemble the absorbance spectra of the adsorbed dyes than the solution spectra. For most of the dyes, a significant contribution from the solution dye would change the action spectra in a noticeable way. For example, in the case of PCCl, contribution from the solution spectra would fill in the valley at 600 nm that is present in both the action spectrum and the spectrum of the adsorbed dye. Second, when the photocurrent response of an electrode without preadsorbed dye is tested following the addition of dye to the electrolyte, the action spectra of the dye does not appear immediately but grows over a period of time. Similarly, when an electrode with an adsorbed dye is exposed to a solution containing a second dye, the spectrum of the second dye does not immediately appear in the action spectrum. Such a case is illustrated in Figure 4c, where the action spectrum is shown for an electrode that was first dyed with DODCI and then tested in a solution containing both DODCI and CCI. Over time, the DODCI spectrum declines and the CCI spectrum appears. Due to the much stronger adsorption of CCI to CuSCN, the DODCI is almost all removed from the surface, leaving a large CCI peak, even though the APCE for DODCI is much higher than that of CCI (Table 1).

In the case of ESABr, the spectrum of the adsorbed dye is red shifted to such an extent, relative to the dye in solution, that the adsorbed dye is probably present in the J-aggregate form. Many cyanine dyes form aggregates known as J-aggregates on the surface of AgX. The peak wavelength of J-aggregates is red shifted by more than 60 nm relative to the monomer.[12] The exact amount of shift depends on the size of the aggregate.[27] The structure of ESA, e.g., the additional conjugated rings on the nuclei, sulfur atoms, and substitution on the 9-carbon all promote J-aggregate formation.[12] In our studies of ESA, the height and position of the peak near 640 nm vary with time and halide ion concentration, relative to the shoulder at 580 nm which corresponds to the adsorbed monomer. The APCE of the shoulder is also noticeably lower than that at the peak, an effect which we attribute to a lower APCE for the adsorbed monomer since adsorbed J-aggregates frequently show different image sensitization efficiencies than adsorbed monomers in photographic applications.[14] The 635 nm peak in the adsorbed PCCl spectrum is probably also that of an aggregate as the height of this peak varies with respect to the other two peaks in the spectrum of adsorbed PCCl.

Because of the high quantum efficiency observed here, a lower bound for the hole injection rate from ESABr to CuSCN can be determined using the fluorescence lifetime of ESABr in various environments. To have high efficiency, the hole injection rate must be faster than all other deactivation channels for the excited dye, the fastest of which will control the observed fluorescence lifetime in the absence of hole injection. For ESABr in ethanol, Welford[28] found a lifetime of 84 ps for the major deactivation channel. Tani et al.[27] found 70 ps in methanol for the monomer, 230 ps for the J-aggregate in water, 26 ps for the J-aggregate adsorbed to SiO_2, and 6 ps for the J-aggregate on AgBr. Assuming the lifetime on SiO_2 is representative of the adsorbed state, roughly applying to the surface of CuSCN, the hole injection rate must be at least on the order of 10^{11} s^{-1}. This lower limit is similar to that found for electron injection into TiO_2 and SnS_2 and provides evidence for the similarity of the two processes.[29] In electron injection, the transfer of the electron from the excited dye orbital into the wide band of empty states above the conduction band edge allows for an apparently activationless reaction.[29] In hole injection, the electron is transferred to an empty dye orbital from a wide band of filled states below the valence band edge. By analogy, the fast reaction rate of hole injection may also be related to a low activation barrier.

Figure 5 shows the photocurrent as a function of potential for several conditions. The photocurrent onset potential in ethanol:$TBABF_4$ depends on the electrode preparation and the dye, yielding values as positive as 400−450 mV vs SCE. The photocurrent begins to saturate at potentials negative of 0 mV and at currents above ~100 μA/cm^2. At 10 times the white light level shown in Figure 5, the photocurrent at −200 mV increases to only 250 μA/cm^2 and rapidly decreases with time. The photocurrent as a function of potential for ESABr in water is also shown in Figure 4. In water, the onset is shifted about 100 mV negative, to +300 mV SCE.

Photocurrent onset occurs at the potential where there is just enough band bending so that an injected hole has some probability of escaping to the bulk (and then being collected in the external circuit) rather than recombining across the surface to the reduced dye or some other electron donor. For a p-type semiconductor, the photocurrent onset potential is less positive than the flat band potential by this amount of band bending.

---

(27) Kemnitz, K.; Yoshihara, K.; Tani, T. *J. Phys. Chem.* **1990**, *94*, 2099.

(28) Welford, D.; Sibbett, W.; Taylor, J. R. *Opt. Commun.* **1980**, *34*, 175.

(29) Willig, F.; Eichberger, R.; Sundaresan, N. S.; Parkinson, B. A. *J. Am. Chem. Soc.* **1990**, *112*, 2702.

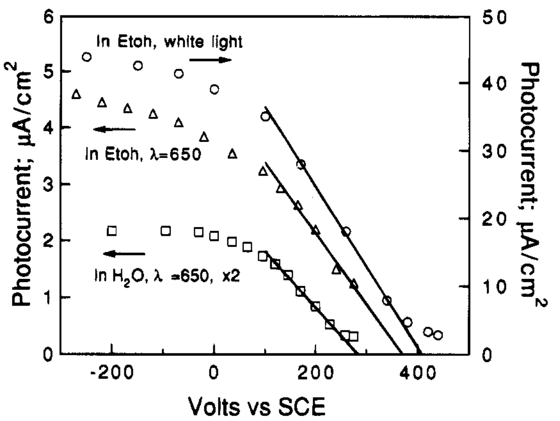

Figure 5. Photocurrent–voltage characteristics of ESABr sensitized CuSCN films. Circles: in ethanol, 0.05 M $TBABF_4$, 10^{-5} M ESABr, 1 mM LiI. White light intensity 5 mW/cm². Triangles: in ethanol, 6 mM LiI, 10^{-4} M ESABr. Monochromatic light intensity 63 μW/cm², $\lambda = 650$ nm, bandpass 10 nm. Squares: H_2O, 0.05 M $HClO_4$, illumination same as for triangles. The lines are least-squares fits through the points on the slope and are included to illustrate the shift in the photocurrent onset with light intensity and solvent.

The photocurrent onset potential thus forms a lower bound for the flat band potential. The flat-band potential in turn is a lower bound for the valence band edge. As our CuSCN films seem to be moderately doped,[9] the Fermi level is expected to be ~100 mV negative of the valence-band edge. A lower bound for the valence band edge of CuSCN in ethanol/$TBABF_4$ is thus around 0.55 V SCE.

In our series of dyes, all dyes with oxidation potentials more positive than 0.7 V vs SCE have APCEs greater than 50% (Table 1). The threshold oxidation potential for high APCE injection lies in the neighborhood of 0.55 V. The low APCE for NCI and CCI are not indicative of weak absorption to the electrode. In both cases, absorption spectra show that the amount of dye adsorbed was equal to or greater than that for ESABr when the same dye concentrations were employed. The threshold for APCE is also related to the valence band edge. Dyes whose excited-state "oxidizing potentials"[30] are less positive than the valence band edge will have no driving force for hole injection. The excited state oxidizing potential for CCI is about 0.35 V more positive than the ground state oxidation potential listed in Table 1,[31] so the 0.55 V threshold potential indicated by Table 1 becomes a threshold potential of 0.9 V in terms of excited-state oxidizing potential. The amount of driving force needed for efficient hole injection is not known. However, assuming it to be at least 0.15 V, the valence band edge is then less positive than 0.75 V vs SCE.[32] The lower limit found using the photocurrent onset and the upper limit just stated indicate that the CuSCN valence band edge in ethanol/TBABF4 is between 0.55 V and 0.75 V SCE.

Concluding Remarks

The fact that weakly adsorbed cyanine dyes can inject holes with high efficiencies suggests that CuSCN can be used as a hole transport layer in a dye-sensitized heterojunction (DSH) solar cell. The weak adsorption of the dyes is relevant because in a TiO_2 DSH the dye will be strongly adsorbed to the TiO_2 and the CuSCN material deposited over the dye layer. The interaction of the CuSCN and the dye will not be "specific" as the orientation of the dye will be fixed by adsorption to the TiO_2. In addition, the +400 mV photocurrent onset potential of the CuSCN electrodes is also located in the appropriate region for application to TiO_2 solar cells as shown schematically in Figure 1. At present, TiO_2 DSPEC cells use the I_3^-/I^- couple in organic solvents such as propylene carbonate or *N*-methyl-2-oxazolidinone.[1] The potential of the iodine couple in these solutions is about +100 mV vs SCE. The open circuit potential of the TiO_2 cells under 1 sun illumination is −700 mV, which implies that the Fermi level in the TiO_2 is near −600 mV SCE.[1,33] Under the best of conditions, the combination of TiO_2 and CuSCN separated by a dye layer should give an open-circuit potential of 1 V. This condition will require that the recombination rate of electrons in TiO_2 and holes in CuSCN, separated by the dye layer, be no faster than the recombination rate for electrons in TiO_2 with iodine in solution. It must be added that the iodine couple has been found to be somewhat unique in giving a very low dark current at TiO_2 and that the open-circuit potential of CuSCN in this study was measured with no intentionally added redox couple.[1,33] Thus the rate of recombination of holes in CuSCN with solution electron donors is not yet known.

The cyanine dyes used in this study do not adsorb to TiO_2 and do not sensitize anodic photocurrent therein, so the question arises whether the dyes which are used in a TiO_2 DSPEC cell can sensitize CuSCN. Ruthenium dyes which sensitize anodic photocurrent in TiO_2 with high efficiency have oxidation potentials generally larger than 0.5 V. The best sensitizer on record has an oxidation potential of 0.85 V.[1,34,35] The excited-state oxidizing potentials of these ruthenium dyes are less positive than their ground-state oxidation potentials, so the excited dyes may not inject holes into CuSCN.[36] However, after an electron has been injected into the TiO_2, it is the ground-state oxidation potential that controls subsequent hole injection into the CuSCN. Thus these ruthenium dyes should be energetically quite capable of sensitizing CuSCN in a TiO_2 DSH cell.

Acknowledgments are made to the Link Energy Foundation, the University of Washington Royalty Research Fund, and to the donors of the Petroleum Research Fund, administered by the American Chemical Society.

CM9500519

---

[30] For ease of expression we use "excited-state oxidizing potential" to refer to the strength of the excited dye as an oxidant. Properly this is called the "excited-state reduction potential", D^*/D^-, i.e., that potential at which the excited state will accept an electron. This is not a measured potential (in our work) and we follow refs 31 and 36 in defining it as the ground-state reduction potential plus the energy of the 0–0 optical transition of the dye. Symmetrically, we use "excited-state reducing potential", defined as the ground-state oxidation potential minus the optical transition energy.

[31] Lenhard, J. *J. Imag. Sci.* **1986**, *30*, 27.

[32] This upper bound is based on oxidation potentials in acetonitrile whereas the photoelectrochemistry was in ethanol. We expect that the oxidation potentials in ethanol are about 50 mV more positive. We have included this adjustment by choosing a slightly lower value for the minimum driving force for efficient injection.

[33] Kay, A.; Humphry-Baker, R.; Gratzel, M. *J. Phys. Chem.* **1994**, *98*, 942.

[34] Nazeeruddin, M. K.; Liska, P.; Moser, J.; Vlachopoulox, N.; Gratzel, M. *Helvtica Chim. Acta* **1990**, *73*, 1788.

[35] Enea, O.; Moser, J.; Gratzel, M. J. *Electroanal. Chem.* **1989**, *259*, 59.

[36] Gouterman, M.; Holten, D. *Photochem. Photobio.* **1977**, *25*, 85.